Biogeochemistry (2024) 167:1281–1295
https://doi.org/10.1007/s10533-024-01174-8

Environmental co-limitation on temperature responses of greenhouse gas production in floodplain sediments

Maidina Zhumabieke · Jinhee Huh · Hyunji Lee · Ji-Hyung Park

Received: 15 April 2024 / Accepted: 12 August 2024 / Published online: 21 August 2024
© The Author(s) 2024

Abstract Despite the rising interest in understanding how climate change could affect the emissions of greenhouse gases (GHGs) from river systems, including floodplains, we still lack a mechanistic understanding of how changing environmental conditions, such as moisture and nutrient availability, limit the temperature responses of GHG production in floodplain sediments. To examine the environmental co-limitations on the temperature responses of three major GHGs (CO_2, CH_4, and N_2O) produced in floodplain sediments, sediments from a constructed wetland on the floodplain of the lower Han River were incubated for 24 d at four temperatures spanning 4–28 ℃, under three conditions (closed, open/wetting, and open/drying). The net production of all three GHGs exhibited nonlinear temperature responses with gas-specific patterns and magnitudes of response varying over the incubation period. During the later incubation phase, positive temperature responses were weakened for the net production of CO_2 and CH_4 in the dried treatments, whereas a similar weakening occurred for N_2O production in the wet treatments. This, combined with incubation-induced changes in dissolved organic carbon and its fluorescence components, indicated the lack or excess of moisture and associated changes in O_2 and organic carbon availability as critical co-limiting factors for the temperature responses of GHG production. Warming decreased $\delta^{13}C$ in the CH_4 emitted from wet and hypoxic sediments, implying a stronger warming effect on CH_4 production over oxidation. Unlike many studies assuming a consistent relationship between temperature and GHG production in sediments irrespective of other environmental conditions, our results suggest that warming effects on the GHG emissions from floodplain sediments would depend on the balance between gas production and consumption under the prevailing constraints of moisture, O_2, and labile carbon availability.

Keywords Climate change · Environmental co-limitation · Greenhouse gases · Oxygen availability · Floodplain sediments · Temperature response

Responsible Editor: Amy M. Marcarelli

Supplementary Information The online version contains supplementary material available at https://doi.org/10.1007/s10533-024-01174-8.

M. Zhumabieke · J. Huh · H. Lee · J.-H. Park (✉)
Department of Environmental Science & Engineering, Ewha Womans University, Seoul 03760, Republic of Korea
e-mail: jhp@ewha.ac.kr

Introduction

Climate change is affecting the behavior of microorganisms in both the water column and sediment of freshwater ecosystems and, consequently, the

emission of greenhouse gases (GHGs) such as CO_2 and CH_4 (Marotta et al. 2014; Jansen et al. 2022). Compared to the extensive studies of climatic effects on GHG emissions from soils (Davidson et al. 1998; Du et al. 2020; Moonis et al. 2021), much less is known about environmental controls on the temperature response (defined as the response of biogeochemical processes to temperature changes) of the production of GHGs in freshwater sediments, including floodplain sediments. Although it has been demonstrated that increasing water temperature can accelerate riverine metabolic processes (Acuña et al. 2008; Marotta et al. 2014), we lack a mechanistic understanding of how concurrent changes in other environmental factors, such as moisture and nutrient availability, modulate warming effects on GHG production in river riparian sediments (Comer-Warner et al. 2018; Wilkinson et al. 2019; Chen et al. 2021).

Recent studies on CO_2 emissions from dried inland waters suggest that the response of CO_2 emissions from the sediments is sensitive to changing water levels by droughts and floodings (Marcé et al. 2019; Keller et al. 2020). The response of CH_4 to warming can be greater than that of CO_2 (Borrel et al. 2011). Annual global CH_4 emissions from streams rivers were estimated at 26.8–27.9 Tg CH_4, which accounts for approximately 15–40% of the emissions from wetlands and lakes (Stanley et al. 2016; Rocher-Ros et al. 2023). Seasonal floodings can deplete O_2 in saturated sediments, creating favorable conditions for anaerobic methanogens producing CH_4 in wetlands that are naturally formed or artificially constructed along floodplains (Sha et al. 2011). Nitrification and denitrification in river sediments are also sensitive to changes in the availability of O_2 and moisture in sediments, generating N_2O as byproducts and hence increasing N_2O emissions from rivers (Chun et al. 2020) and surrounding wetlands (Ruser et al. 2006). Although numerous individual studies have investigated climatic effects on the production of GHGs in river and wetland sediments, there has been limited research comparing the differential temperature responses of the three GHGs.

More frequent occurrences of extreme hydrological events due to climate change can increase water level fluctuations and their associated environmental impacts on floodplains. Changing sediment moisture levels and the consequent alterations in O_2 availability can either enhance or moderate the temperature sensitivity of GHG emissions from floodplain sediments. However, few studies have examined the combined effects of temperature, moisture, and O_2 on GHG production in floodplain sediments. We conducted laboratory incubation experiments with sediment samples from a constructed wetland on the floodplain of the lower Han River. The primary objectives were as follows: (1) to compare the temperature responses of the net production of CO_2, CH_4, and N_2O in the floodplain sediments, and (2) to elucidate how the availability of moisture and O_2 constrains the temperature responses of the three GHGs. We hypothesized that gas production in floodplain sediments would vary depending on the GHG type, with differential responses to temperature increases depending on the prevailing environmental conditions. Specifically, we expected that wetting and drying would induce either positive or negative effect on the temperature response of the net production of CO_2, CH_4, and N_2O in floodplain sediments, depending on the shifting optimal ranges of moisture and O_2 availability for involved microbial processes including methanogenesis, CH_4 oxidation, nitrification, and denitrification.

Material and methods

Study site and sampling

In April 2022, floodplain sediment samples were collected at a constructed wetland of the Gangseo Marsh Ecological Park (latitude: 37° 35′ 11.46″; longitude: 126° 49′ 07.76″; elevation: 7 m) on the floodplain of the lower Han River (Fig. S1). The total area of the Gangseo Marsh Ecological Park is 0.37 km^2, including 537 m^2 of sandy shoreline along the Han River and 3,225 m^2 of floodplains interspersed with several interconnected constructed wetlands that receive inflow water from the Han River. The artificial freshwater wetlands are dominated by reeds (*Phragmites communis*), Amur silver grasses (*Miscanthus sacchariflorus*), and Korean willows (*Salix pierotii*) along the waterways surrounded by gently sloped river banks planted with various deciduous trees (Seoul Metropolitan Government. 2022).

Floodplain sediment samples and water from the river channel were collected at three randomly selected sites (S1, S2, and S3; Fig. S1). The primary

goal of this collection was not to measure sediment GHG production rates under the exact field conditions, but instead to obtain enough representative sediments to use in incubation experiments. At three randomly chosen locations within each site, a metal shovel was used to collect sediment samples within the wetland adjacent to the channel, with depth ranging from 5 to 20 cm below the surface. Large leaves and roots were discarded and the remaining sediments from three sampling points were immediately composited into a 1 L amber glass bottle without empty space to minimize sediment exposure to the air. During the sediment sampling, the water temperature, pH, conductivity, and dissolved oxygen (DO) were measured using a portable multi-parameter water quality probe (Orion 5-Star Portable; Thermo Scientific, USA). A portable weather sensor (Watchdog 1650 Micro Station; Spectrum Technologies, USA) was used to measure the air temperature, air pressure, and humidity.

The three bottles of sediment from three sites were transported on ice before being stored in a 4 °C refrigerator in the laboratory. The sediment samples from the three sites were composited into a homogenized sample within one week. Before initiating the incubation experiment, any remaining debris including stones, plant debris, and living organisms which could significantly affect the measurement of the net GHG production were removed from the sediment samples. To minimize air exposure while homogenizing the samples, we removed only the easily recognizable items and then gently mixed the remaining sediment inside a closed plastic bag as quickly as possible.

Lab incubation experiment

The experiment included three sediment conditions to examine the temperature responses of GHG production in floodplain sediments with varying levels of moisture and O_2. Equal volumes (60 mL) of the homogenized sediment samples from the three sampling sites were placed in 120 mL amber serum bottles to initiate the experiment. In the "Closed" treatment, air exchange was prevented by sealing the incubation bottles immediately with butyl rubber stoppers and aluminum crimp caps to create anoxic conditions in the sediment. The headspace of each bottle was sparged with ultrapure He gas to induce anoxic condition over the course of the 24-d incubation. The "Closed" treatment may create conditions that are not representative of GHG production in actual floodplain sediments, but it was included as a reference to compare against the other sediment condition treatments. In the wetting ("Open_wet") and drying ("Open_dry") treatments, the incubation bottles remained unsealed to allow for free air exchange as in the field. Ultrapure water was added to the Open_wet treatment every 3–4 d to maintain a constant moisture level in the saturated sediments by keeping the total weight of each sampling bottle at the initial level, whereas no water was added to the Open_dry treatment to simulate drying sediment conditions. Three replicates of the three sediment condition treatments were incubated at the four temperatures (4 ℃, 12 ℃, 20 ℃, and 28 ℃), for a total of 36 experimental units. The incubation was conducted in the dark at four temperature-controlled incubators. In each incubator, the incubation bottles of the three treatments were randomly located on the same level with a minimal variation from the set temperature. The experiment was incubated for 24 days to examine temporal changes in the temperature response of the net GHG production.

For eight repeated measurements of net production rates of the three GHGs (1st, 2nd, 4th, 6th, 10th, 14th, 19th, and 24th days), the bottles of the Open_wet and Open_dry treatments were first flushed with He and then sealed for a 1-h incubation, while headspace samples (20 mL) were directly taken from the sealed bottles of the Closed treatments by displacing them with the same volume of He. Immediately after completing the final gas sampling on Day 24, DO was measured in the sediment using a multi-parameter probe (Orion 5-Star Portable; Thermo Scientific USA), and then 10 g of sediment sample was mixed with 100 mL of ultrapure water in 250 mL polycarbonate bottles on a shaker for 30 min to extract organic matter (OM) and inorganic nutrients from the sediments, following Robertson et al. (1999).

Water and sediment analysis

The water samples collected from the three sampling sites (n = 3) and the sediment extracts from the incubation experiment (n = 36) were filtered through pre-combusted 0.7 μm glass fiber filters (GF/F, Whatman, USA). The filters were dried at

60 ℃ for 48 h and weighed to measure total suspended solids (TSS). The concentration of dissolved organic carbon (DOC) in the filtrate was measured using a total organic carbon (TOC) analyzer (TOC-V_{CPH}; Shimadzu, Japan) with the limit of detection lower than 0.01 mg C mg L^{-1}. Major ions were measured using an ion chromatograph (883 Basic IC plus; Metrohm, Switzerland) with the limits of detection: 0.03 mg L^{-1} for NH_4^+, 0.02 mg L^{-1} for NO_3^-, and 0.01 mg L^{-1} for PO_4^{3-}. The same QA/QC procedures were employed for all water analyses to ensure analytical quality. Standards with known concentrations as well as blank samples consisting of ultrapure water were analyzed for every batch of 10 samples to examine instrumental stability and analytical precision. Relative standard deviations of the replicate analyses were lower than 5%.

Sediment extracts were also measured for ultraviolet–visible (UV–Visible) absorbance across a wavelength range of 200–1,100 nm using a UV–Vis spectrophotometer (8453; Agilent, USA) and fluorescence excitation-emission matrices (EEMs) using a fluorescence spectrophotometer (F7000; Hitachi, Japan). Fluorescence EEMs were obtained by scanning at 5-nm intervals across excitation wavelengths of 200–400 nm and at 1-nm intervals across emission wavelengths of 290–540 nm (Begum et al. 2019). The EEMs measured for the initial sediment extracts prior to the incubation were subtracted from those for the final sediment extracts from the last day to provide visual representation of incubation-induced changes in major fluorescent components. The EEMs were further used to identify major fluorescent organic components using parallel factor analysis (PARAFAC) in MATLAB (R2022b, Mathworks, Natick, USA) with the DOM Fluor toolbox developed by Stedmon and Bro (2008). The fluorescence components were validated by visual inspection of the residuals and split-half analysis. The two components identified by PARAFAC modeling were termed "humic-like" (peak intensity at 300/433 nm, ex/em) and "protein-like" (275/340 nm, ex/em) based on the peak wavelengths reported in the literature (Fellman et al. 2010). Incubation-induced changes in the maximum fluorescence intensities of the two identified components were compared across the four incubation temperatures among the three treatments.

Gas analysis

During the eight gas samplings, a 20 mL gas sample was collected from the headspace (60 mL) of the incubation bottle using a 50 mL syringe with a three-way stopcock. The syringe was flushed five times with He prior to the sampling. The air pressure and temperature were measured in the room for the calculation of the partial pressures and dissolved concentrations of the three GHGs based on Henry's law (Hudson 2004). The gas samples were simultaneously analyzed for CO_2, CH_4, and N_2O using a gas chromatograph (GC 7890A; Agilent, USA). The GC was equipped with a 12 ft 1/8 inch Supelco Hayesep Q column, a flame ionization detector (FID) coupled with a methanizer for CH_4 and CO_2, and a microelectron capture detector (μECD) for N_2O. The GC was operated following the routine settings and QA/QC procedures described in detail by Jin et al. (2018). Standard gases of the three GHGs in N_2 balance, together with ultrapure N_2 gases as blanks, were measured for every batch of ten samples. The precision of the replicate analyses was typically lower than 5%.

To examine differential warming effects on the production and consumption of CH_4 under the three different incubation conditions, gas samples taken from the Closed and Open_wet treatments on Day 24 were further analyzed for the stable carbon isotope ratio of CH_4 to elucidate the source of CH_4 production using a GasBench-IRMS (ThermoScientific, Bremen, Germany) at the UC Davis Stable Isotope Facility. The stable C isotope composition is expressed as $\delta^{13}C = (R_{sample}/R_{standard})-1$, where R_{sample} and $R_{standard}$ are the ratios of heavy to light isotopes (^{13}C:^{12}C) in the sample and standard (Vienna Pee Dee Belemnite), respectively. The stable C isotope composition has widely been used to evaluate the potential sources and transformations of CH_4 in wetland sediments and various aquatic ecosystems. Source tracing is based on the deviations of the measured values of $\delta^{13}C$ in the CH_4 from the usual ranges found for the CH_4 generated by acetoclastic (−70 to −32‰) and hydrogenotrophic (−115 to −55‰) methanogenesis (Hornibrook et al. 2000; Wells et al. 2020).

Data presentation and analysis

To compare treatment effects, the net production of each GHG was calculated from the concentration increase in headspace, normalized per day and per unit volume of sediment (for instance, expressed as mg CO_2 L^{-1} d^{-1}). The cumulative production of the three GHGs in the experimental treatments was also interpolated throughout the incubation period from the eight daily production rates (Park et al. 2002).

Temperature quotient or coefficient (Q_{10}) was calculated as a measure of temperature sensitivity based on the net gas production rates measured at four temperatures. The relationship between temperature and GHG production rates was nonlinear, as often found in other studies (e.g., Wilkinson et al. 2019). Therefore, Q_{10} was calculated using the following exponential equations (Lloyd and Taylor 1994; Moonis et al. 2021):

$$R = ae^{bT}$$

where R represents the rate of respiration at temperature T and a and b are constants.

$$Q_{10} = e^{10b}$$

Significant treatment effects were analyzed using one-way analysis of variance (ANOVA) followed by Tukey's test for multiple comparisons using SPSS Statistics 26 (IBM Inc., USA). Prior to statistical analyses, data distribution was examined using the Shapiro–Wilk normality test. In the case of skewed data, log-transformed data were used for further analyses. The relationships between GHG production rates and environmental variables were examined by performing principal component analysis (PCA) using the "FactoMineR" and "factoextra" packages in R (version 4.2.2). Correlations between factors for each treatment group were visualized using the package "corrplot" operating in R (version 4.2.2). Regressions between temperature and net GHG production rates were analyzed using SigmaPlot 15.0 (Systat Software Inc., UK).

Results

Eight gas samplings conducted during the 24-d incubation period revealed large variations in the daily net production (the flux representing the difference between production and consumption) of the three GHGs over time and between treatments (Fig. 1). Overall, the net production rates of CO_2 and N_2O tended to be highest in the Open_wet treatments, followed by those of the Open_dry and Closed treatments, whereas the CH_4 production rate was distinctively higher in the Closed and Open_wet treatments at the highest temperature, compared to the generally low levels found in the Open_dry treatments throughout the incubation (Table 1). In the Closed treatments, the net production rates of CO_2 and N_2O were low throughout the incubation period, whereas the net CH_4 production continued to increase at the highest temperature, reaching levels comparable to those in the Open_wet treatments on Day 24 (Fig. 2). The Open_wet and Open_dry treatments displayed large variations in CO_2 and N_2O production rates during the second half of the incubation, particularly due to fluctuations at 28 °C under which moisture levels can change more quickly. For instance, the repeated wettings at 3–4 day intervals in the Open_wet treatments resulted in fluctuations in the net CO_2 production ranging from 62 to 2112 mg CO_2 L^{-1} d^{-1} (Table 1).

The cumulative production of the three GHGs widely varied with temperature and treatment (Fig. S2). The cumulative production rates of CO_2 and N_2O were highest at 28 °C in the Open_wet treatments, followed by those of the Open_dry treatments. Although the difference was not statistically significant, the cumulative amount (2,112 mg CO_2 L^{-1}) produced in the Open_wet treatments at 28 °C was 20 times greater than that of the Closed treatments. The cumulative N_2O production in the Open_wet and Open_dry treatments amounted to 2,360 µg N_2O L^{-1} and 1,766 µg N_2O L^{-1} at 28 °C, respectively. In contrast, the CH_4 production in the Closed treatments at 28 °C exceeded that of the Open_wet treatments, reaching 24,344 µg CH_4 L^{-1} on Day 24. The cumulative CH_4 production in the Open_dry treatments was as low as 1,242 µg CH_4 L^{-1} at the highest temperature.

To examine temporal changes in gas-specific temperature responses, the daily net production of the

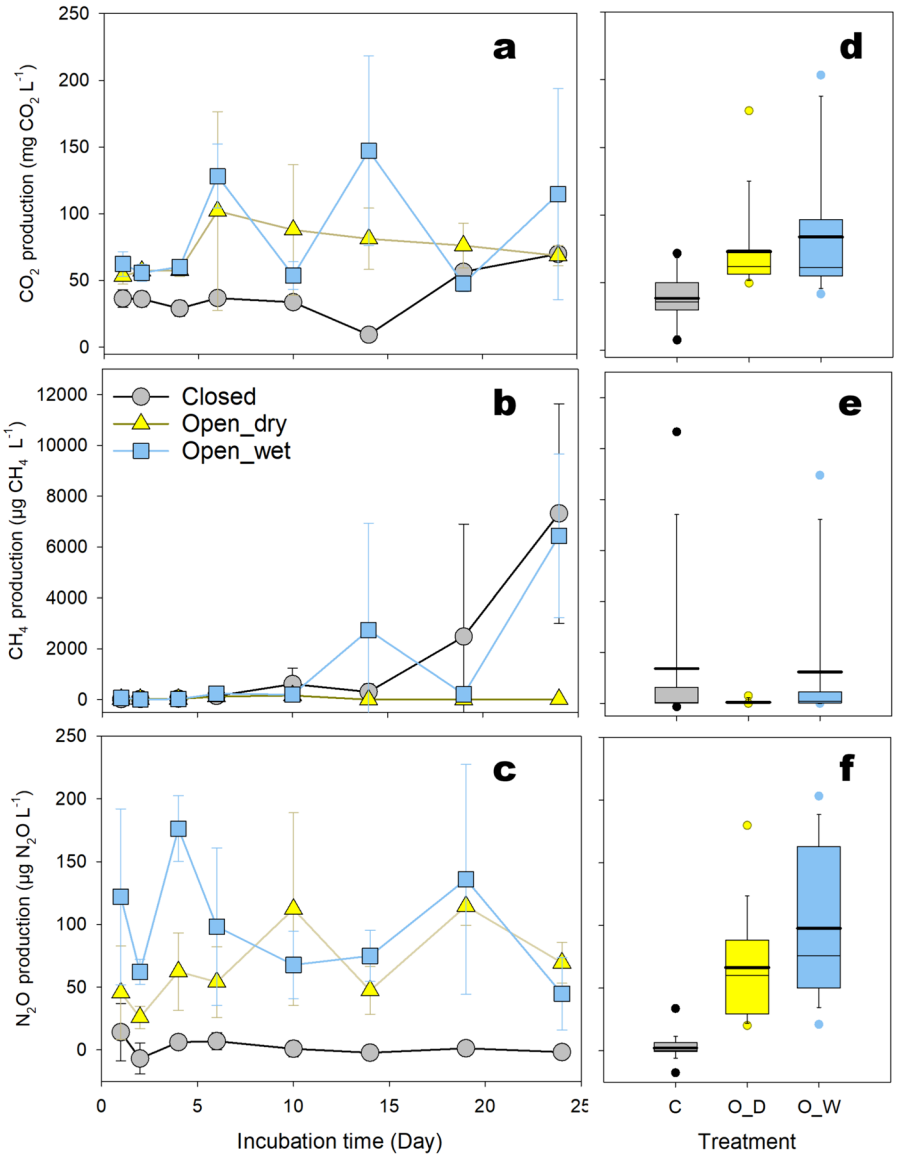


Fig. 1 Net production of three greenhouse gases in floodplain sediments during 24-day incubation. Sediments were incubated at four temperatures spanning 4–28 ℃ under Closed (C; anoxic), Open_dry (O_D; open to atmosphere without water amendment), and Open_wet (O_W; open to atmosphere with water amendment) conditions. Eight measurements are expressed either as the means ± one standard deviation (four temperatures) of daily net production (mg or µg L^{-1} d^{-1}) of **a** CO_2, **b** CH_4, and **c** N_2O or the corresponding boxplots showing the pooled data of **d** CO_2, **e** CH_4, and **f** N_2O. Thick and thin horizontal lines represent means and medians, respectively

three GHGs was compared across the four incubation temperatures for three selected days, each representing the initial, mid-term, and final state of the incubation: Days 1, 10, and 24 (Fig. 2). Statistics from the nonlinear regressions between temperature and net gas production rates measured on Day 24, along with Q_{10} values, are summarized in Table S1. On all three days, net CO_2 production showed similar nonlinear increases with increasing temperature in all three treatments (Fig. 2). However, the strongest temperature response at 28 °C shifted from the Open_dry treatments on Day 10 to the Open_wet treatments on Day 24. The temperature responses of net N_2O production were maintained within a relatively narrow range, with the strongest response occurring at 28 °C and switching from the Open_wet (Day 1) to Open_dry treatments (Days 10 and 24) (Fig. 2).

Although net CH_4 production also generally displayed positive temperature responses in all treatments except the Open_dry treatments on Day 24, the strongest temperature responses were found in the Closed and Open_wet treatments at 28 °C and continued to increase over time by more than 100-fold on Day 24, compared to the rather weak responses

Table 1 Mean net production rates of CO_2 (mg m^{-1} d^{-1}), CH_4 (μg L^{-1} d^{-1}), and N_2O (μg L^{-1} d^{-1}) during 24-day incubation of floodplain sediments at four temperatures spanning 4–28 ℃

Temperature	CO_2 (mg L^{-1} d^{-1})			CH_4 (μg L^{-1} d^{-1})			N_2O (μg L^{-1} d^{-1})		
	Closed	Open_dry	Open_wet	Closed	Open_dry	Open_wet	Closed	Open_dry	Open_wet
4 ℃	52^{Aa} (8–134)	191^{Aa} (19–441)	208^{Aa} (25–489)	5.38^{Aa} (1–13)	18.5^{Aa} (−2 to 31)	22^{Ba} (−2 to 36)	3^{Aa} (0–7)	12^{Ba} (1–20)	8^{Aa} (0.6–13)
12 ℃	95.5^{Aa} (12–239)	253^{Aa} (28–585)	263^{Aa} (27–621)	36.6^{Aa} (6–73)	24.7^{Aa} (5–65)	15^{Aa} (−2to 39)	7^{Aa} (0.0–28)	16^{Ba} (7–24)	17^{Ba} (7–25)
20 ℃	138^{Aa} (20–309)	397^{Aa} (34–1063)	356^{Aa} (37–849)	9.4^{Aa} (4–14)	132^{Ba} (12–413)	60^{Aa} (41–88)	17^{Aa} (2–54)	173^{Ba} (32–526)	143^{Aa} (25–402)
28 ℃	332^{Ab} (37–849)	762^{Ab} (53–1899)	848^{Ab} (62–2112)	4557^{Ab} (10–24344)	610^{Ab} (24–1242)	5683^{Ab} (67–23,031)	25^{Ab} (6–41)	630^{Ab} (45–1766)	994^{Bb} (121–2360)

Treatments include Closed, Open_wet, and Open_dry. Values are the means of eight repeated measurements over the course of 24-day incubation, followed by minimum and maximum in parentheses (n = 8). Values followed by different capital letters are significantly different between treatments for the same temperature at $P < 0.05$. Values followed by different lowercase letters are significantly different between temperatures for the same treatment at $P < 0.05$

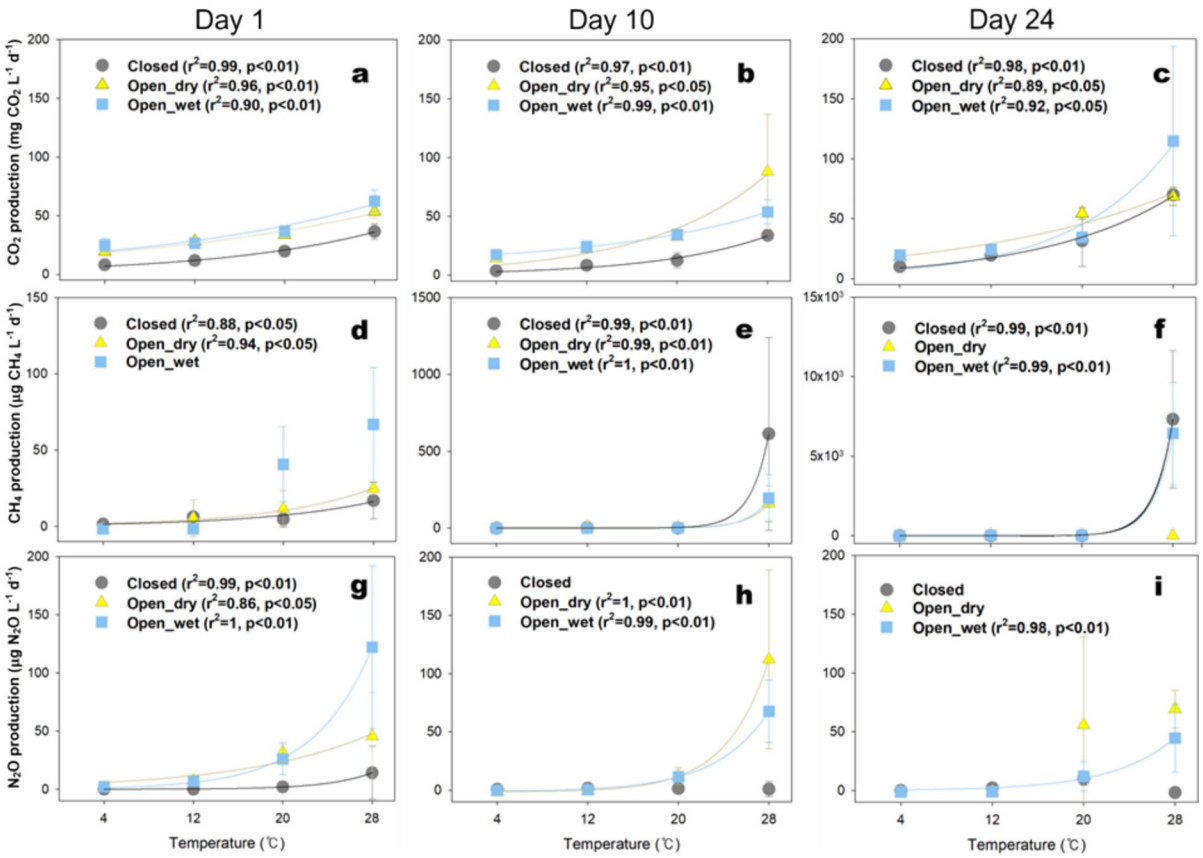


Fig. 2 Changing temperature responses of the net production of three greenhouse gases during the 24-day incubation period of floodplain sediments. Data are presented for three selected days (Day 1: **a**, **d**, **g**; Day 10: **b**, **e**, **h**; Day 24: **c**, **f**, **i**) and three treatments including Closed, Open_dry, and Open_wet. Error bars represent ± one standard deviation (n = 3). Only significant regressions are indicated by the best-fit regression lines (exponential growth model). Note the increase in y-axis range for CH_4 production from (**d**) Day 1 to (**e**) Day 10 to (**f**) Day 24

observed on Day 1. In contrast, the net CH_4 production was extremely low in the Open_dry treatments across all temperatures on Day 24. The values of $\delta^{13}C$ in CH_4 taken from the Closed and Open_wet treatments on Day 24 provided some insights into the potential sources of CH_4 in the sediments incubated under different magnitudes of warming (Table 2). The mean of $\delta^{13}C$ in CH_4 from the Closed treatments was lower at 28 ℃ (−47.49 ± 4.28‰) than those measured at 12 ℃ (−31.76 ± 2.37‰) and 20 ℃ (−31.73 ± 9.54‰), although the differences were statistically not significant. The mean of the $\delta^{13}C$ values measured in the Open_wet treatments at 28 ℃ was the lowest (−52.96 ± 12.40‰). The $\delta^{13}C$ values measured in the Closed and Open_wet treatments under 28 ℃ fall in the ranges found for the CH_4 generated by acetoclastic (−70 to −32‰) and hydrogenotrophic (−115 to −55‰) methanogenesis (Hornibrook et al. 2000; Wells et al. 2020).

Table 2 $\delta^{13}C$ in CH_4 released from the Closed and Open_wet sediments on Day 24

Treatment	$\delta^{13}C$ (‰)		
	12 ℃	20 ℃	28 ℃
Closed	−31.76 (2.37)	−31.73 (9.54)	−47.49 (4.28)
Open_wet			−52.96 (12.40)

Values are presented as means followed by standard deviations in parentheses (n = 3)

During the 24-d incubation period, the mean values of DO tended to decrease in both the Closed and Open_wet treatments, although the generally low DO values were not significantly different among the treatments (Table 3). In the Open_dry treatments, NO_3^--N concentrations in the sediment extracts tended to increase in proportion to temperature. However, DOC concentrations significantly declined with temperature, reflecting warming-enhanced biodegradation of DOC into CO_2, which was indicated by the relatively high cumulative CO_2 production measured at 28 ℃ (Fig. S2). The nutrients measured in the sediment extracts of the Open_wet and Closed treatments exhibited relatively small changes compared to the initial nutrient levels (NO_3^-–N: 4–37%; PO_4^{3-}: 9–17%; Table 3). However, DOC concentrations in the extracts of the Closed and Open_wet treatments significantly increased in proportion to temperature increases (Table 3).

Changes in fluorescence EEMs and two identified PARAFAC components over the 24-d incubation also revealed distinct differences in the DOM composition of sediment extracts between the Open_dry and the other wetter and hypoxic treatments (Fig. 3). In

Table 3 Concentrations of DO, DOC, and three ions that were measured initially (0 h) and following 24 days (Day 24) of incubation of floodplain sediments

Treatments	Temperature	DO (mg L^{-1})	DOC (mg L^{-1})	NH_4^+–N (mg L^{-1})	NO_3^- (mg L^{-1})	SO_4^{2-} (mg L^{-1})	PO_4^{3-} (mg L^{-1})
Sediment (0 h)	4 ℃	0.88	24.5	0.65	0.52	5.37	1.73
Closed (Day 24)	4 ℃	0.15 (0.06)^{Aa}	22.1 (1.7)^{Aa}	0.54 (0.09)^{Aa}	0.38 (0.06)^{Aa}	5.09 (0.24)^{Aa}	1.52 (0.06)^{Aa}
	12 ℃	0.22 (0.13)^{Aa}	25.2 (0.9)^{Ab}	0.79 (0.04)^{Ab}	0.34 (0.02)^{Aa}	4.24 (0.41)^{Aa}	1.58 (0.03)^{Aa}
	20 ℃	0.15 (0.06)^{Aa}	28.7 (1.1)^{Ac}	1.01 (0.03)^{Ac}	0.38 (0.03)^{Aa}	3.79 (0.12)^{Aa}	1.45 (0.06)^{Aa}
	28 ℃	0.06 (0.01)^{Aa}	29.9 (0.4)^{Ac}	1.71 (0.14)^{Ad}	0.38 (0.07)^{Aa}	3.85 (0.14)^{Aa}	1.58 (0.05)^{Aa}
Open_dry (Day 24)	4 ℃	0.35 (0.16)^{Aa}	22.5 (1.0)^{Aa}	0.44 (0.08)^{Aa}	0.38 (0.08)^{Aa}	5.50 (0.35)^{Aa}	1.42 (0.07)^{Aa}
	12 ℃	0.23 (0.13)^{Aa}	23.5 (0.2)^{Ab}	0.69 (0.05)^{Ab}	0.49 (0.27)^{Aa}	5.49 (0.24)^{Aa}	1.42 (0.11)^{Aa}
	20 ℃	2.05 (1.50)^{Aa}	20.9 (0.7)^{Bc}	0.25 (0.08)^{Bb}	0.73 (0.31)^{Aa}	11.25 (0.77)^{Aa}	0.09 (0.01)^{Bb}
	28 ℃	8.31 (3.60)^{Aa}	20.9 (1.7)^{Bc}	0.35 (0.14)^{Ba}	3.06 (4.71)^{Aa}	16.37 (10.83)^{Aa}	0.50 (0.38)^{Bb}
Open_wet (Day 24)	4 ℃	0.28 (0.07)^{Aa}	23.1 (0.5)^{Aa}	0.60 (0.06)^{Aa}	0.50 (0.28)^{Aa}	5.94 (0.68)^{Aa}	1.43 (0.11)^{Aa}
	12 ℃	0.31 (0.29)^{Aa}	24.2 (1.3)^{Aa}	0.71 (0.08)^{Aa}	0.35 (0.03)^{Aa}	5.13 (0.65)^{Aa}	1.47 (0.01)^{Aa}
	20 ℃	0.09 (0.01)^{Aa}	29.6 (0.2)^{Ab}	1.00 (0.02)^{Aa}	0.33 (0.06)^{Aa}	3.98 (0.02)^{Aa}	1.51 (0.03)^{Aa}
	28 ℃	0.03 (0.01)^{Aa}	27.8 (1.5)^{Ab}	1.12 (0.42)^{Bb}	0.43 (0.15)^{Aa}	4.30 (0.40)^{Aa}	1.58 (0.16)^{Aa}

Values are means followed by standard deviations in parentheses (n = 3). Values followed by different uppercase letters are significantly different among the treatments at $P < 0.05$, while values followed by different lowercase letters are significantly different among the four temperatures at $P < 0.05$

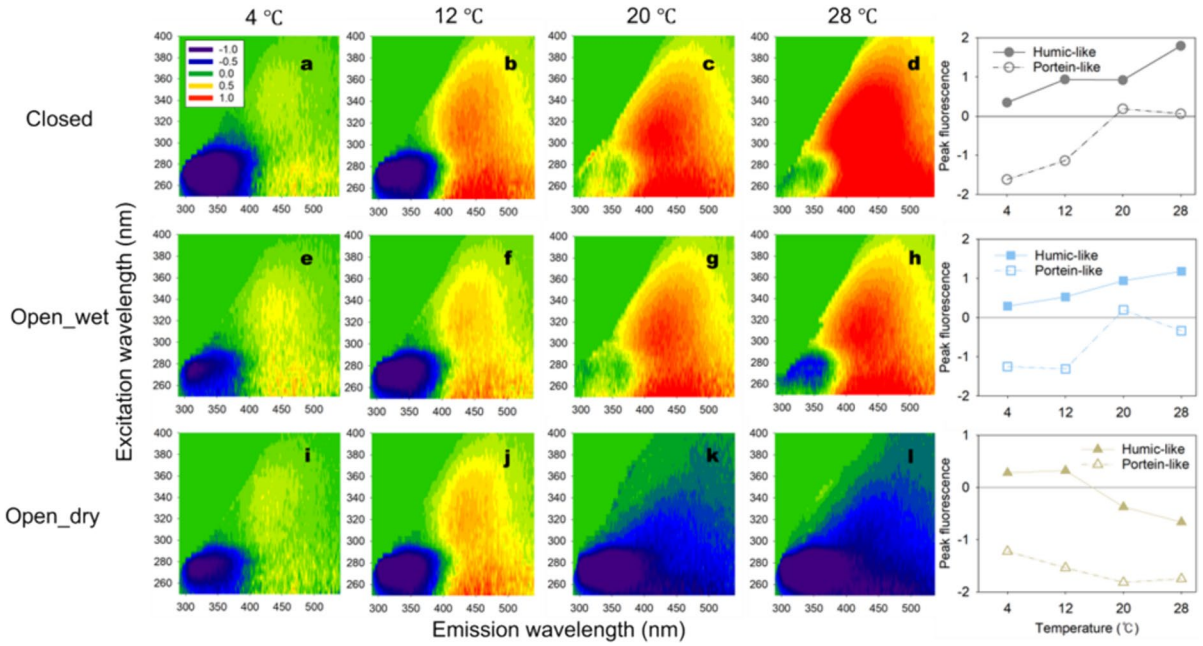


Fig. 3 Changes in fluorescence excitation-emission matrices (EEMs) and intensities of two identified fluorescent components over the 24-day incubation of Closed (**a**–**d**), Open_wet (**e**–**h**), and Open_dry (**i**–**l**) treatments. Incubation temperature: 4 °C (**a**, **e**, **i**), 12 °C (**b**, **f**, **j**), 20 °C (**c**, **g**, **k**), and 28 °C (**d**, **h**, **l**). The differential EEMS for the first of three replicates per treatment were obtained by subtracting the initial EEMs measured for the sediment extracts prior to the incubation from those for the extracts on the last day. The humic-like fluorescence peak at 300/433 nm (Ex/Em) and the protein-like fluorescence peak at 275/340 nm (Ex/Em) were identified by the parallel factor analysis (PARAFAC)

agreement with the warming-enhanced color (blue) changes in the differential EEMs of the Open_dry treatments, the peak fluorescence intensity of both the humic-like (at 300/433 nm, ex/em) and protein-like (at 275/340 nm, ex/em) PARAFAC components decreased in proportion to temperature increases. Both the Closed and Wet_open treatments exhibited the reversed patterns: warming-induced red color shifts in the differential EEMs and increases in fluorescence intensities of both PARAFAC components.

The PCA biplot displays close relationships between two GHGs (CO_2 and CH_4) and temperature and some water quality components (DOC NH_4^+, and PO_4^{3-}) for both the Closed and Open_wet treatments (Fig. 4). The three water quality variables (DOC NH_4^+, and PO_4^{3-}), temperature, and the two GHGs (CO_2 and CH_4) constituted the three largest contributing variables to the two identified principal components (Dim1 and Dim2; axis loadings reported in Table S2). These relationships were consistent with the significant positive correlations between the two GHGs (CO_2 and CH_4) and temperature, DOC, and NH_4^+ measured in the Closed and Open_wet treatments, although the significance level was weak or lacking for some relationships in the Open_wet treatment (Fig. 5). In the Open_dry treatment, N_2O was clearly separated from NO_3^-, SO_4^{2-}, and DO (Fig. 4), which was consistent with positive, but not significant correlations between N_2O and the same components (Fig. 5).

Discussion

Although the temperature dependence of GHG production has been examined for various sediment types (Marotta et al. 2014; Shelley et al. 2015; Comer-Warner et al. 2018), this study is unique in simultaneously comparing the predominant environmental controls on the temperature responses of the net production of the three GHGs in floodplain sediments. Gas-specific temperature responses observed during the 24-d incubation suggest that warming effects on the net production of the three GHGs

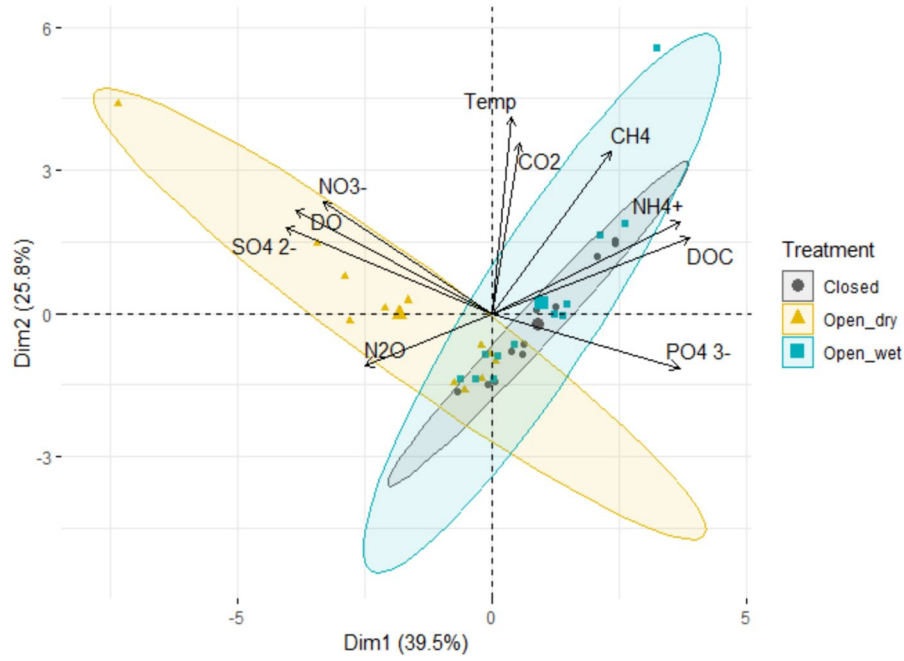


Fig. 4 Biplots comparing the contributing variables identified by principal component analysis (PCA) of data from the three treatments of floodplain sediments: Closed, Open_dry (open to atmosphere), and Open_wet (open to atmosphere and wetted). Temp indicates temperature, while Dim1 and Dim2 denote the primary and secondary principal components, respectively

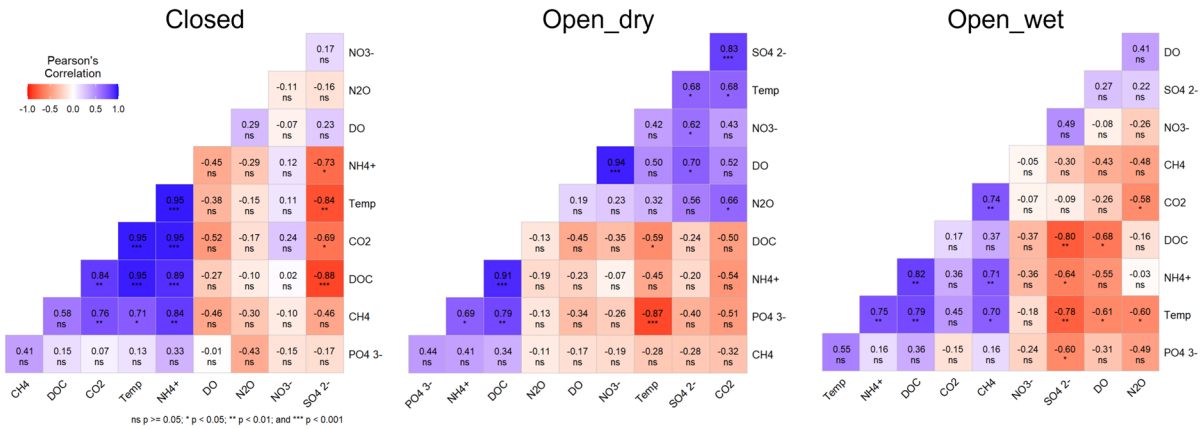


Fig. 5 Correlations between the net production rates of GHGs and water quality components in the sediment extracts measured on the last day of 28-d incubation of the Closed, Open_dry, and Open_wet treatments. Positive and negative correlations are indicated by blue and red colors, respectively, with significance levels denoted by either ns (not significant) or asterisks ($^{*}P<0.05$; $^{**}P<0.01$; $^{***}P<0.001$). Temp indicates temperature

can be modulated by other prevailing environmental factors including O_2, moisture, and labile DOC availability (Figs. 1, 2). In particular, the weakened later-stage responses in the Open_dry (CH_4) and Open_wet (N_2O) treatments (Fig. 2) without exhibiting any depletion of major nutrients such as nitrogen (Table 3), suggest a lack or excess of moisture and associated changes in O_2 availability as the primary co-limiting factors. While assessing the gas-specific warming effects on GHG production in floodplain sediments, we discuss the predominant co-limiting factors for the temperature responses of the three GHGs. Additional discussion is then provided regarding the implications of the research findings for predicting riverine GHG emissions under a changing climate.

Environmental controls on the differential temperature responses of three GHGs

The nonlinear positive relationships between temperature and net CO_2 production found in all three treatments agreed with previous incubation experiments with lake sediments (Marotta et al. 2014) and river bottom sediments (Shelley et al. 2015; Comer-Warner et al. 2018). However, the exponential temperature responses persisted only in the Open_wet treatments (Fig. 2), indicating the role of moisture as a primary control on the temperature responses of CO_2 production. As moisture becomes a critical factor limiting microbial respiration in the drying sediment, moisture loss can negatively affect the respiratory response to warming (Carey et al. 2016).

The strong temperature dependence of the net CH_4 production in the Closed and Open_wet treatments (Fig. 2; Table S1) suggests that moisture is also critical for the temperature response of CH_4 production in floodplain sediments. The rate of CH_4 production in freshwater systems generally increases exponentially with temperature (Brooks Avery et al. 2003). The divergence of the temperature responses between the Open_dry and the other two, wetter treatments (Fig. 3) corroborates the significance of the moisture level for methanogenesis in flooded sediments. This finding is in line with the negative relationship between water table depth and the temperature dependence of CH_4 emissions from 204 wetlands compiled by a global synthesis (Chen et al. 2021). Increased water temperature stimulates microbial activity but reduces the dissolution of gases in water, which can enhance the physical process of CH_4 evasion from the water column to the atmosphere (Soumis et al. 2004; Schrier-Uijl et al. 2011).

The values of $\delta^{13}C$ in the CH_4 emitted from the floodplain sediments indicated the role of methanogenic archaea in CH_4 production at higher temperatures. This observation agrees with an isotopic signature averaging −42.3‰ that was linked to acetoclastic methanogenesis as the primary mechanism for CH_4 production in freshwater wetlands (Hornibrook et al. 2000). The isotope ratio alone cannot provide direct evidence for a warming effect on methanogenesis over CH_4 oxidation, because temperature-enhanced CH_4 oxidation can simultaneously enrich the isotopic signature (Whiticar 1999; Jin et al. 2018; Park et al. 2023). However, the warming effect on CH_4 oxidation appeared much weaker than that on CH_4 production in the Closed and Open_wet treatments, potentially due to oxygen-depleted sediment conditions prevailing at the end of the incubation period (DO levels ranging from 0.03 to 0.3 mg L^{-1}). Oxygen availability may explain the unique temperature-response curves of CH_4 given differential warming effects on CH_4 production and oxidation under hypoxic conditions (Shelley et al. 2015). CH_4 production by methanogenic archaea is increasingly hindered by rising O_2 levels (Ragsdale and Kumar 1996; Borrel et al. 2011), resulting in a negative relationship between DO levels and CH_4 emissions from flooded sediments (Schrier-Uijl et al. 2011).

High concentrations of easily decomposable DOC can stimulate the production of CH_4 in streamwater and sediments (Keller and Stallard 1994; Crawford and Stanley 2016; Romeijn et al. 2019). Based on incubation experiments with bottom sediments from lowland agricultural streams, Romeijn et al. (2019) suggested both the quantity and quality (as indicated by OM aromaticity) of DOC as the primary controls over microbial metabolic activity and the production of CO_2 and CH_4. The decreases in DOC concentrations and fluorescence intensities of the protein-like and humic-like PARAFAC components in the Open_dry treatments concurred with commensurate increases in CO_2 and little changes in CH_4. Together, these trends indicate warming-enhanced aerobic consumption of labile DOC that might not have been replenished from the diminishing pool under the drying conditions. The Open_wet treatments produced more CO_2 and CH_4 at higher DOC concentrations under warmer conditions. These results, combined with the significant correlations between the two GHGs (CO_2 and CH_4) and DOC (Fig. 5), imply that the production of CO_2 and CH_4 can be stimulated in saturated floodplain sediments when anoxic conditions are coupled with a sustained supply of labile OM until the organic pool reaches a threshold for depletion. The warming-enhanced fluorescence intensities in both the protein-like and humic-like peaks identified for the DOM extracted from the Closed and Open_wet treatments support the sustained DOM supply within the 24-d time frame that might be before reaching the depletion threshold. OM-rich sediments tend to be more reactive to warming, as shown by the OM-dependent temperature responses of streambed sediments (Comer-Warner et al. 2018).

Compared to CO_2 and CH_4, N_2O displayed the most complex temperature response patterns, as illustrated by the large fluctuations of the net N_2O production in the Closed and Open_wet treatments during the later incubation phase (Fig. 2). These complex temperature responses may reflect the narrow range of suitable conditions for the net N_2O production linked to various N transformation processes. Complete nitrification and denitrification can occur under optimal conditions, namely oxic and anoxic conditions, respectively. However, varying amounts of N_2O can be produced from incomplete nitrification and denitrification under suboptimal conditions of moisture and O_2 availability. Whereas the net N_2O production in the Closed treatments was low under high moisture and anoxic conditions that might be optimal for complete denitrification, varying amounts of N_2O were produced in both Open_dry and Open_wet treatments at the higher temperatures (20 °C and 28 °C) throughout the 24-d incubation period. These results emphasize the varying potentials of N_2O production in the floodplain sediments under changing conditions of moisture and O_2.

The varying environmental conditions away from the narrow optimal range for nitrification and denitrification may explain the lack of straightforward relationships between N_2O production and key controlling factors, as also found in a global meta-analysis on the temperature sensitivity of freshwater denitrification and N_2O production (Velthuis and Veraart 2022). Prior studies found that the activity of microorganisms containing the *nosZ* gene responsible for reduction of N_2O to N_2 might decrease with increasing temperature beyond the threshold at 25 ℃, producing more N_2O (Liao et al. 2018; Chang et al. 2022). As the drastic increases in the net N_2O production of the Open_dry treatments at the highest two temperatures (20 ℃ and 28 ℃) illustrate, warming around and beyond 25 ℃, coupled with the narrow range of suitable levels of moisture and O_2, can tip the balance between the production and consumption toward an N_2O surge.

Implications for riverine greenhouse gas emissions under a changing climate

The gas-specific temperature responses observed during the 24-d incubation suggest that warming can increase CO_2 production in floodplain sediments under a wide range of moisture and O_2 availability, whereas warming effects on the net production of CH_4 and N_2O would depend on the complex interplay between production and consumption under a relatively narrow range of optimal moisture and O_2 conditions. The extremely high Q_{10} values estimated for the Closed and Open_wet floodplain treatments (Table S1) imply that warming effects on the net production of CH_4 in floodplain sediments can become stronger under saturated conditions accompanied by hypoxic to anoxic conditions. However, prolonged drying conditions may reverse CH_4 production under the negative influence of oxic conditions on methanogenesis while temporarily enhancing N_2O production from nitrification or denitrification under shifting O_2 conditions.

As a result of climatic warming, it has been projected that river water temperatures will increase by 0.8–1.6 °C for 2071–2100 relative to 1971–2000 (van Vliet et al. 2013). Although experimental and modeling studies have reported either linear or exponential temperature responses of CO_2 and CH_4 production in lake sediments (Marotta et al. 2014; Yvon-Durocher et al. 2014; Jansen et al. 2022), temperature responses have been found to differ between CO_2 and CH_4 production in streambed sediments, with nonlinear CH_4 responses primarily explained by differential temperature effects on CH_4 production and oxidation (Shelley et al. 2015; Comer-Warner et al. 2018). These studies have usually focused on the responses of CH_4 relative to CO_2. For example, Shelley et al. (2015) found that the temperature response of CH_4 production was twice that of anaerobic CO_2 production. Our results suggest that varying moisture and O_2 conditions can significantly modulate warming effects on the net production of both CH_4 and N_2O in floodplain sediments to a degree unexpected for CO_2 production. The Q_{10} values for CO_2 varied little among the treatments (Table S1) compared to those for CH_4 and N_2O. Wetting combined with exposure to air increased the Q_{10} for N_2O by a factor of 6.9 relative to that of the Closed treatments. These results indicate a significant contribution of warming-enhanced GHG production in floodplain sediments with varying moisture and O_2 levels to the riverine emissions of GHGs.

The combined effects of warming and wetting can enhance GHG emissions from sediments more than the rates expected from the isolated effects

of temperature and moisture changes (Yang et al. 2022). This coupled effect was initially verified in the Open_wet treatments. When the floodplain sediments were sufficiently moist under completely (Closed) or temporarily (Open_wet) anoxic conditions, the large increases in CH_4 production (reaching around 5,000 μg L^{-1} d^{-1}) at the highest incubation temperature resulted in the extremely high Q_{10} values (Closed: 403; Open_wet: 330). After O_2 and alternative electron acceptors have been depleted, the ensuing anaerobic state creates a favorable condition for production of CH_4 (Kuivila et al. 1989). A similar effect of water levels on the temperature dependence of CH_4 production in wetland soils has been established by a global synthesis (Chen et al. 2021). When the floodplain sediment was dried, a greater rate of CO_2 production followed during a sustained drought period, similar to the continuously declining CO_2 production we observed in the Closed treatments in this study. Paranaíba et al. (2020) studied a situation of extreme droughts followed by heavy rainfalls, where CO_2 emission increased while sediment dried over 15 days, then decreased when the sediment was completely dry. Although further experiments in the field would be required to corroborate the findings from the laboratory incubation experiment described here, the temporal changes in drying and wetting effects on GHGs we found suggest that more frequent occurrences of droughts and floodings would result in higher rates of GHG production under actual field conditions.

In summary, warming has the potential to enhance the net production of GHGs in floodplain sediments and its contribution to the riverine GHG emissions, but under the constraints of varying environmental conditions. The specific outcome would depend on the prevailing environmental conditions represented by moisture and O_2 levels. As a caveat for extrapolating the results of this study, it should be emphasized that laboratory incubation experiments are limited in simulating actual field conditions. For instance, fluctuating river flows would result in more frequent exchange of substances between the river water and interacting sediments. Under field conditions, elevated water temperatures can have a larger or smaller effect on the actual rates of GHG production as affected by the intervening influences of material exchange on prevailing sediment conditions. More field-based measurements of GHG emissions across a wide range of temperatures and moisture conditions are required to provide reliable estimates of emission increases in response to future temperature increases.

Conclusions

A 24-d incubation experiment revealed gas-specific temperature responses of the net production of three GHGs in floodplain sediments that are constrained by co-limiting factors including moisture, O_2, and labile organic carbon. The CO_2 production in the floodplain sediments responded positively to warming over a wide range of moisture and O_2. The significance of O_2 as the key co-limiting factor was evident in the production of CH_4. The net CH_4 production in the dried sediments gradually decreased owing to the increase in O_2, whereas a drastic increase in CH_4 production occurred in the Open_wet and Closed treatments at the highest temperature under increasingly anoxic conditions with a constant supply of labile carbon. The strongest temperature response of the N_2O production shifted from the wetted treatments to the dried treatments during the later incubation phase, implying that a narrow range of optimal hypoxic conditions for nitrogen transformation processes (either nitrification or denitrification) generating N_2O varies with time depending on moisture and O_2 availability. The gradual drying combined with the active interaction of bare sediments with air may be responsible for the greater flux of N_2O compared to the wetter treatments. Overall, the results suggest that warming effects on riverine emissions of the three GHGs would be significantly affected by the changing availability of moisture and O_2 that can shift the balance between gas production and consumption in floodplain sediments. In the face of intensifying hydrologic extreme events, more frequent occurrences of droughts and floodings can significantly alter the temperature responses of GHG emissions from floodplain sediments by affecting the co-limiting environmental factors.

Acknowledgements We gratefully acknowledge that Jinhee Huh made a significant contribution to initiating and conducting this study prior to a fatal accident during a field trip. We also thank Ms. Sunghee Choi for her help with laboratory work. Two anonymous reviewers and Dr. Amy Marcarelli provided constructive comments that helped us improve the manuscript.

Author contributions Conceptualization: [Ji-Hyung Park], [Maidina Zhumabieke]; Investigation [Maidina Zhumabieke], [Jinhee Huh], [Hyunji Lee]; Writing–Original Draft: [Maidina Zhumabieke], [Ji-Hyung Park]; Writing–Review & Editing: [Ji-Hyung Park], Funding Acquisition: [Ji-Hyung Park].

Funding This study was funded by National Research Foundation of Korea, including NRF-2017R1D1A1B06035179, Ji-Hyung Park, 2021M316A1091270, Ji-Hyung Park, Maidina Zhumabieke, and Hyunji Lee, and Brain Korea 21 FOUR Program "REFINANCE: Research and Education team For an Integrated Approach on Newly emerging Contaminants in multiple Environmental media" at the Department of Environmental Science & Engineering, Ewha Womans University, Ji-Hyung Park, Maidina Zhumabieke, and Hyunji Lee.

Data availability Data are available and can be requested from the corresponding author (jhp@ewha.ac.kr).

Declarations

Conflict of interest The authors declare that they have no conflicts of interest.

Open Access This article is licensed under a Creative Commons Attribution-NonCommercial-NoDerivatives 4.0 International License, which permits any non-commercial use, sharing, distribution and reproduction in any medium or format, as long as you give appropriate credit to the original author(s) and the source, provide a link to the Creative Commons licence, and indicate if you modified the licensed material. You do not have permission under this licence to share adapted material derived from this article or parts of it. The images or other third party material in this article are included in the article's Creative Commons licence, unless indicated otherwise in a credit line to the material. If material is not included in the article's Creative Commons licence and your intended use is not permitted by statutory regulation or exceeds the permitted use, you will need to obtain permission directly from the copyright holder. To view a copy of this licence, visit http://creativecommons.org/licenses/by-nc-nd/4.0/.

References

Acuña V, Wolf A, Uehlinger U, Tockner K (2008) Temperature dependence of stream benthic respiration in an Alpine river network under global warming. Freshw Biol 53:2076–2088. https://doi.org/10.1111/j.1365-2427.2008.02028.x

Begum MS, Jang I, Lee J-M et al (2019) Synergistic effects of urban tributary mixing on dissolved organic matter biodegradation in an impounded river system. Sci Total Environ 676:105–119. https://doi.org/10.1016/j.scitotenv.2019.04.123

Borrel G, Jézéquel D, Biderre-Petit C et al (2011) Production and consumption of methane in freshwater lake ecosystems. Res Microbiol 162:832–847. https://doi.org/10.1016/j.resmic.2011.06.004

Brooks Avery G, Shannon RD, White JR et al (2003) Controls on methane production in a tidal freshwater estuary and a peatland: methane production via acetate fermentation and CO_2 reduction. Biogeochemistry 62:19–37. https://doi.org/10.1023/A:1021128400602

Carey JC, Tang J, Templer PH et al (2016) Temperature response of soil respiration largely unaltered with experimental warming. Proc Natl Acad Sci U S A 113:13797–13802. https://doi.org/10.1073/pnas.1605365113

Chang B, Yan Z, Ju X et al (2022) Quantifying biological processes producing nitrous oxide in soil using a mechanistic model. Biogeochemistry 159:1–14. https://doi.org/10.1007/s10533-022-00912-0

Chen H, Xu X, Fang C et al (2021) Differences in the temperature dependence of wetland CO_2 and CH_4 emissions vary with water table depth. Nat Clim Chang 11:766–771. https://doi.org/10.1038/s41558-021-01108-4

Chun Y, Kim D, Hattori S et al (2020) Temperature control on wastewater and downstream nitrous oxide emissions in an urbanized river system. Water Res 187:116417. https://doi.org/10.1016/j.watres.2020.116417

Comer-Warner SA, Romeijn P, Gooddy DC et al (2018) Thermal sensitivity of CO_2 and CH_4 emissions varies with streambed sediment properties. Nat Commun 9:2803. https://doi.org/10.1038/s41467-018-04756-x

Crawford JT, Stanley EH (2016) Controls on methane concentrations and fluxes in streams draining human-dominated landscapes. Ecol Appl. https://doi.org/10.1890/15-1330.1

Davidson EA, Belk E, Boone RD (1998) Soil water content and temperature as independent or confounded factors controlling soil respiration in a temperate mixed hardwood forest. Glob Chang Biol 4:217–227. https://doi.org/10.1046/j.1365-2486.1998.00128.x

Du Y, Wang Y-P, Su F et al (2020) The response of soil respiration to precipitation change is asymmetric and differs between grasslands and forests. Glob Chang Biol 26:6015–6024. https://doi.org/10.1111/gcb.15270

Fellman JB, Hood E, Spencer RGM (2010) Fluorescence spectroscopy opens new windows into dissolved organic matter dynamics in freshwater ecosystems: a review. Limnol Oceanogr 55:2452–2462. https://doi.org/10.4319/lo.2010.55.6.2452

Hornibrook ERC, Longstaffe FJ, Fyfe WS (2000) Factors influencing stable isotope ratios in CH_4 and CO_2 within subenvironments of freshwater wetlands: implications for δ-signatures of emissions. Isotopes Environ Health Stud 36:151–176. https://doi.org/10.1080/10256010008032940

Hudson F (2004) Sample preparation and calculations for dissolved gas analysis in water samples using a GC headspace equilibration technique, RSKSOP-175, (Revision No 2). U.S. Environmental Protection Agency, Washington, pp 1–14

Jansen J, Woolway RI, Kraemer BM et al (2022) Global increase in methane production under future warming of lake bottom waters. Glob Chang Biol 28:5427–5440. https://doi.org/10.1111/gcb.16298

Jin H, Yoon TK, Begum MS et al (2018) Longitudinal discontinuities in riverine greenhouse gas dynamics generated by dams and urban wastewater. Biogeosciences 15:6349–6369. https://doi.org/10.5194/bg-15-6349-2018

Keller M, Stallard RF (1994) Methane emission by bubbling from Gatun Lake, Panama. J Geophys Res 99:8307. https://doi.org/10.1029/92JD02170

Keller PS, Catalán N, von Schiller D et al (2020) Global CO_2 emissions from dry inland waters share common drivers across ecosystems. Nat Commun 11:2126. https://doi.org/10.1038/s41467-020-15929-y

Kuivila KM, Murray JW, Devol AH, Novelli PC (1989) Methane production, sulfate reduction and competition for substrates in the sediments of Lake Washington. Geochim Cosmochim Acta 53:409–416. https://doi.org/10.1016/0016-7037(89)90392-X

Liao R, Miao Y, Li J et al (2018) Temperature dependence of denitrification microbial communities and functional genes in an expanded granular sludge bed reactor treating nitrate-rich wastewater. RSC Adv 8:42087–42094. https://doi.org/10.1039/C8RA08256A

Lloyd J, Taylor JA (1994) On the temperature dependence of soil respiration. Funct Ecol 8:315. https://doi.org/10.2307/2389824

Marcé R, Obrador B, Gómez-Gener L et al (2019) Emissions from dry inland waters are a blind spot in the global carbon cycle. Earth Sci Rev 188:240–248. https://doi.org/10.1016/j.earscirev.2018.11.012

Marotta H, Pinho L, Gudasz C et al (2014) Greenhouse gas production in low-latitude lake sediments responds strongly to warming. Nat Clim Chang 4:467–470. https://doi.org/10.1038/nclimate2222

Moonis M, Lee J-K, Jin H et al (2021) Effects of warming, wetting and nitrogen addition on substrate-induced respiration and temperature sensitivity of heterotrophic respiration in a temperate forest soil. Pedosphere 31:363–372. https://doi.org/10.1016/S1002-0160(20)60069-8

Paranaíba JR, Quadra G, Josué IIP et al (2020) Sediment drying-rewetting cycles enhance greenhouse gas emissions, nutrient and trace element release, and promote water cytogenotoxicity. PLoS ONE 15:e0231082. https://doi.org/10.1371/journal.pone.0231082

Park J-H, Kalbitz K, Matzner E (2002) Resource control on the production of dissolved organic carbon and nitrogen in a deciduous forest floor. Soil Biol Biochem 34:813–822. https://doi.org/10.1016/S0038-0717(02)00011-1

Park J-H, Lee H, Zhumabieke M, Kim S-H, Shin K-H, Khim B-K (2023) Basin-specific pollution and impoundment effects on greenhouse gas distributions in three rivers and estuaries. Water Res 236:119982. https://doi.org/10.1016/j.watres.2023.119982

Ragsdale SW, Kumar M (1996) Nickel-containing carbon monoxide dehydrogenase/Acetyl-CoA synthase. Chem Rev 96:2515–2540. https://doi.org/10.1021/cr950058+

Robertson GP, Sollins P, Ellis BG, Lajtha K (1999) Exchangeable ions, pH, and cation exchange capacity. Standard soil methods for long-term ecological research. Oxford University Press, New York, pp 109–111

Rocher-Ros G, Stanley EH, Loken LC et al (2023) Global methane emissions from rivers and streams. Nature 621:530–535. https://doi.org/10.1038/s41586-023-06344-6

Romeijn P, Comer-Warner SA, Ullah S et al (2019) Streambed organic matter controls on carbon dioxide and methane emissions from streams. Environ Sci Technol 53:2364–2374. https://doi.org/10.1021/acs.est.8b04243

Ruser R, Flessa H, Russow R et al (2006) Emission of N_2O, N_2 and CO_2 from soil fertilized with nitrate: effect of compaction, soil moisture and rewetting. Soil Boil Biochem 38:263–274. https://doi.org/10.1016/j.soilbio.2005.05.005

Schrier-Uijl AP, Veraart AJ, Leffelaar PA et al (2011) Release of CO_2 and CH_4 from lakes and drainage ditches in temperate wetlands. Biogeochemistry 102:265–279. https://doi.org/10.1007/s10533-010-9440-7

Seoul Metropolitan Government (2022) Gangseo Hangang Park. https://hangang.seoul.go.kr/archives/342

Sha C, Mitsch WJ, Mander Ü et al (2011) Methane emissions from freshwater riverine wetlands. Ecol Eng 37:16–24. https://doi.org/10.1016/j.ecoleng.2010.07.022

Shelley F, Abdullahi F, Grey J, Trimmer M (2015) Microbial methane cycling in the bed of a chalk river: oxidation has the potential to match methanogenesis enhanced by warming. Freshw Biol 60:150–160. https://doi.org/10.1111/fwb.12480

Soumis N, Duchemin É, Canuel R, Lucotte M (2004) Greenhouse gas emissions from reservoirs of the western United States. Global Biogeochem Cy 18:GB3022. https://doi.org/10.1029/2003GB002197

Stanley EH, Casson NJ, Christel ST et al (2016) The ecology of methane in streams and rivers: patterns, controls, and global significance. Ecol Monogr 86:146–171. https://doi.org/10.1890/15-1027

Stedmon CA, Bro R (2008) Characterizing dissolved organic matter fluorescence with parallel factor analysis: a tutorial. Limnol Oceanogr Methods 6:572–579. https://doi.org/10.4319/lom.2008.6.572

van Vliet MTH, Franssen WHP, Yearsley JR et al (2013) Global river discharge and water temperature under climate change. Glob Environ Change 23:450–464. https://doi.org/10.1016/j.gloenvcha.2012.11.002

Velthuis M, Veraart AJ (2022) Temperature sensitivity of freshwater denitrification and N_2O emission—a meta-analysis. Global Biogeochem Cy 36:e2022GB007339. https://doi.org/10.1029/2022GB007339

Wells NS, Chen J-J, Maher DT, Huang P, Erler DV, Hipsey M, Eyre BD (2020) Changing sediment and surface water processes increase CH_4 emissions from human-impacted estuaries. Geochim Cosmochim Acta 280:130–147

Whiticar MJ (1999) Carbon and hydrogen isotope systematics of bacterial formation and oxidation of methane. Chem Geol 161:291–314. https://doi.org/10.1016/S0009-2541(99)00092-3

Wilkinson J, Bodmer P, Lorke A (2019) Methane dynamics and thermal response in impoundments of the Rhine River, Germany. Sci Total Environ 659:1045–1057. https://doi.org/10.1016/j.scitotenv.2018.12.424

Yang J, Jia X, Ma H et al (2022) Effects of warming and precipitation changes on soil GHG fluxes: A meta-analysis. Sci Total Environ 827:154351. https://doi.org/10.1016/j.scitotenv.2022.154351

Yvon-Durocher G, Allen AP, Bastviken D et al (2014) Methane fluxes show consistent temperature dependence across microbial to ecosystem scales. Nature 507:488–491. https://doi.org/10.1038/nature13164

Publisher's Note Springer Nature remains neutral with regard to jurisdictional claims in published maps and institutional affiliations.